

# Magnetic-polaron-driven magnetoresistance in the pyrochlore $\text{Lu}_2\text{V}_2\text{O}_7$

H. D. Zhou,<sup>1,2</sup> E. S. Choi,<sup>2</sup> J. A. Souza,<sup>3</sup> J. Lu,<sup>2</sup> Y. Xin,<sup>2</sup> L. L. Lumata,<sup>1,2</sup> B. S. Conner,<sup>1,2</sup> L. Balicas,<sup>2</sup> J. S. Brooks,<sup>1,2</sup> J. J. Neumeier,<sup>3</sup> and C. R. Wiebe<sup>1,2,\*</sup>

<sup>1</sup>*Department of Physics, Florida State University, Tallahassee, Florida 32306-3016, USA*

<sup>2</sup>*National High Magnetic Field Laboratory, Florida State University, Tallahassee, Florida 32306-4005, USA*

<sup>3</sup>*Department of Physics, Montana State University, Bozeman, Montana 59717-3840, USA*

(Received 6 November 2007; published 28 January 2008)

The structural, magnetic, and transport properties of single-crystalline  $\text{Lu}_2\text{V}_2\text{O}_7$  are studied.  $\text{Lu}_2\text{V}_2\text{O}_7$  shows a ferromagnetic transition at  $T_C=69.5$  K and a negative magnetoresistance (MR) as high as 50% at  $T_2=75$  K with an applied field of 5 T. Through various experiments, it is demonstrated that the mechanism for MR is not through double exchange, but through a polaron-mediated behavior similar to  $\text{Ti}_2\text{Mn}_2\text{O}_7$ . This places  $\text{Lu}_2\text{V}_2\text{O}_7$  as the only other example of polaron-mediated MR among the pyrochlore oxides.

DOI: [10.1103/PhysRevB.77.020411](https://doi.org/10.1103/PhysRevB.77.020411)

PACS number(s): 75.50.Dd, 61.05.cp, 75.30.Cr, 75.47.Gk

Colossal magnetoresistance (CMR) materials have attracted a lot of attention due to their potential technological applications.<sup>1</sup> Well-studied materials of this class are the hole-doped perovskite manganates  $\text{La}_{1-x}\text{Sr}_x\text{MnO}_3$  and  $\text{La}_{1-x}\text{Ca}_x\text{MnO}_3$ .<sup>2,3</sup> In the manganites, a double-exchange (DE) interaction between  $\text{Mn}^{3+}$  and  $\text{Mn}^{4+}$  is believed to stabilize the ferromagnetism and the compounds show metallic behavior below the magnetic transition ( $T_C$ ). One of the key characteristics of CMR manganites is a Jahn-Teller distortion of the  $\text{MnO}_6$  octahedra.

Recently, a study of materials with frustrated sublattices and strong magnetoresistance has been brought to the forefront of this field. CMR has been discovered in the pyrochlore  $\text{Ti}_2\text{Mn}_2\text{O}_7$  (Refs. 4–6) and Cr-based chalcogenide spinels.<sup>7</sup> These materials are believed to have a different mechanism of CMR compared to the manganite systems—there is no structural anomaly associated with the magnetoresistance, and there are other differences in the magnetic properties. The DE model is not suitable in materials such as  $\text{Ti}_2\text{Mn}_2\text{O}_7$  due to its single-valent  $\text{Mn}^{4+}$  and relatively weak spin-charge and spin-lattice couplings.<sup>8</sup> Majumdar and Littlewood (ML) have developed a model predicting that the magnetoresistance in low-carrier-density ferromagnets depends on the carrier density, and for ultralow densities, the carriers will self-trap as magnetic polarons.<sup>9,10</sup> Magnetoresistance measurements for  $\text{Ti}_2\text{Mn}_{2-x}\text{Ru}_x\text{O}_7$  confirm that  $\text{Ti}_2\text{Mn}_2\text{O}_7$  sits in this regime.<sup>11</sup>

The pyrochlore  $\text{Lu}_2\text{V}_2\text{O}_7$  is isostructural to  $\text{Ti}_2\text{Mn}_2\text{O}_7$  with a single-valent  $\text{V}^{4+}$ . Previous studies have shown this sample to be a ferromagnetic semiconductor<sup>12,13</sup> with  $T_C \approx 70$  K. The reported zero-field resistivity data show typical semiconductor behavior without any anomaly but the application of light can induce a metal-insulator transition.<sup>14</sup> It is well known that the sample's quality is important for transport measurements and grain boundary effect can easily smear out the intrinsic properties. Motivated by the analogy between  $\text{Lu}_2\text{V}_2\text{O}_7$  and  $\text{Ti}_2\text{Mn}_2\text{O}_7$ , we explored the possibility of magnetoresistance in  $\text{Lu}_2\text{V}_2\text{O}_7$ . In this Rapid Communication, we prepared high-quality single-crystalline  $\text{Lu}_2\text{V}_2\text{O}_7$ . The detailed structural, magnetic, transport data on this sample show a negative magnetoresistance as high as 50% with an applied field of  $H=5$  T around 75 K. We show

in this work that  $\text{Lu}_2\text{V}_2\text{O}_7$  is the only other known example of a pyrochlore with strong magnetoresistance, and we verify that the theory of Majumdar and Littlewood can be used to describe the MR within a framework of polaron formation as opposed to the double-exchange mechanism.

Single crystals of  $\text{Lu}_2\text{V}_2\text{O}_7$  were grown by the traveling-solvent floating-zone (TSFZ) technique. The x-ray powder diffraction (XRD) patterns were recorded by a HUBER Imaging Plate Guinier Camera 670 with  $\text{Cu } K\alpha_1$  radiation. XRD patterns down to 10 K were obtained with a He compressor. The XRD data were fit using the program FULLPROF with typical  $R_p \approx 7.0$ ,  $R_{wp} \approx 8.0$ , and  $\chi^2 \approx 1.8$ . X-ray Laue diffraction was used to confirm the quality of the crystal. The thermal expansion was measured with a capacitive dilatometer cell constructed from fused quartz. Susceptibility measurements were made with a Quantum Design superconducting quantum interference device (SQUID) magnetometer. The specific heat measurements were performed on a PPMS (physical property measurement system, Quantum Design). The resistivity was measured by a four-probe technique. The thermal conductivity  $\kappa(T)$  was measured with a steady-state heat-flow technique.

The room-temperature XRD pattern shows that the sample is single phase with a cubic,  $Fd-3m$ , structure, retained down to 10 K [Fig. 1(a)]. The temperature dependence of the lattice parameter (extracted through Rietveld refinements using FULLPROF) shows no anomalies over the measured temperature region. The thermal expansion coefficient only shows a tiny anomaly associated with the ferromagnetic transition ( $\Delta\alpha=2.9 \times 10^{-7}/\text{K}$ ) as expected for a thermodynamic probe.

The Curie-Weiss fitting for the inverse of the high-temperature susceptibility ( $1/\chi$ ) on  $\text{Lu}_2\text{V}_2\text{O}_7$  with  $H=5$  T [Fig. 2(a)] yields  $\theta=106$  K and  $\mu_{eff}=1.75\mu_B$ . The saturated magnetic moment [Fig. 2(b)] is  $M_{sat}=1.0\mu_B$ . These values agree with the anticipated values for a localized  $\text{V}^{4+}$  ( $3d^1$ ) electron ( $\mu_{eff}=1.73\mu_B$ ,  $S=1/2$ ). The value of  $\theta=106$  K also agrees with the reported value for a stoichiometric sample.<sup>15</sup> The susceptibility measured with a low field of 50 Oe shows a sharp transition with a  $T_C \approx 70$  K [inset of Fig. 2(a)].

Previous resistivity measurements on  $\text{Lu}_2\text{V}_2\text{O}_7$  demonstrated that the sample is a semiconductor with a thermal

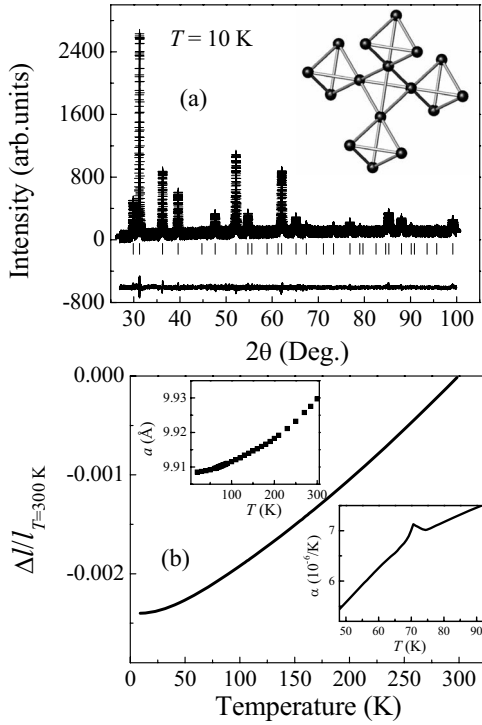


FIG. 1. (a) XRD pattern for  $\text{Lu}_2\text{V}_2\text{O}_7$  (plus marks) at 10 K. The solid curves are the best fits from the Rietveld refinement using FULLPROF. The vertical marks indicate the position of Bragg peaks, and the bottom curves show the difference between the observed and calculated intensities. Inset: the crystal structure for  $\text{Lu}_2\text{V}_2\text{O}_7$ . (b) Thermal expansion coefficient along the  $a$  direction for  $\text{Lu}_2\text{V}_2\text{O}_7$ . Top inset: temperature dependence of lattice parameter from x-ray measurements. Bottom inset: detail of the thermal expansion coefficient near the ferromagnetic transition at 70 K.

activation energy around 200 meV.<sup>14</sup> Our magnetoresistance measurements on high-quality single-crystalline  $\text{Lu}_2\text{V}_2\text{O}_7$  show several surprising features: (i) the slope of the zero-field resistivity  $\rho(T)$  changes from negative to positive below 75 K [Fig. 3(a)] and then changes back to negative again below 60 K. This drop of resistivity below 75 K indicates a discrete transition between two electronic states. (ii) With a small field of  $H=2$  T, the cusp around 75 K almost disappears and the data show a negative MR, which arrives at a maximum value  $\rho(2T)/\rho(0)-1=-0.3$  at 75 K [Fig. 3(b)]. (iii) The negative MR behavior is peaked only at 75 K.

The MR  $= -0.5$  with a field of  $H=5$  T [Fig. 3(b)] is comparable to the value reported for pyrochlore  $\text{Tl}_2\text{Mn}_2\text{O}_7$ .<sup>5</sup> Within our resolution, there is only a tiny structural anomaly ( $\delta\alpha=2.9\times 10^{-7}/\text{K}$ ) associated with the ferromagnetic transition and the magnetoresistance around 70 K. This is clearly different from the  $\text{La}_{1-x}\text{Ca}_x\text{MnO}_3$  compounds which have an abrupt volume change (around 0.13%) at the magnetic phase transition.<sup>16</sup> The coupling between this large structural distortion and the charge carriers due to the mixed  $\text{Mn}^{3+}/\text{Mn}^{4+}$  valence is a key signature for CMR in the perovskite manganites.<sup>17</sup> This model is not suitable for  $\text{Lu}_2\text{V}_2\text{O}_7$  with single-valent  $\text{V}^{4+}$  and weak spin-charge-lattice couplings.

As shown in Fig. 3(c), the resistivity between 80 K and 160 K can be described by the Mott variable-range hopping (VRH) model:

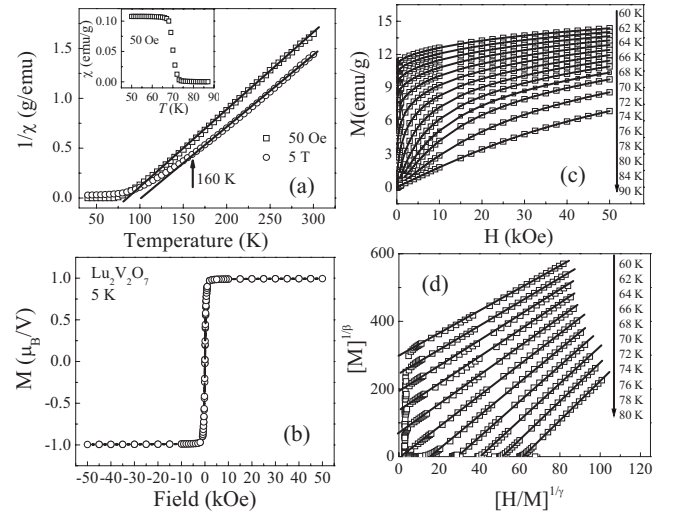


FIG. 2. (a) Temperature dependences of the inverse of the susceptibility measured with applied field as 50 Oe and 5 T, (b)  $M$ - $H$  curves at 5 K, (c)  $M$ - $H$  curves at several temperatures around 70 K, and (d) modified Arrott plot isotherms for the optimum fitting. Inset of (a): susceptibility measured with 50 Oe around 70 K for  $\text{Lu}_2\text{V}_2\text{O}_7$ .

$$\rho = A \exp[(T_0/T)^{1/4}]. \quad (1)$$

This is expected for a low-density semiconductor. However, it is unusual that the VRH model provides a good fit to the data only below 160 K. We suggest that this temperature represents the beginning of polaron formation (marked by an anomaly in the power law of the resistivity). Furthermore, the resistivity measured below 5 T shows less pronounced activated behavior, which indicates that the binding energy of the magnetic polarons is reduced under an applied field. According to the ML model, for low-carrier-density ferromagnets, the self-trapped carriers could behave as magnetic

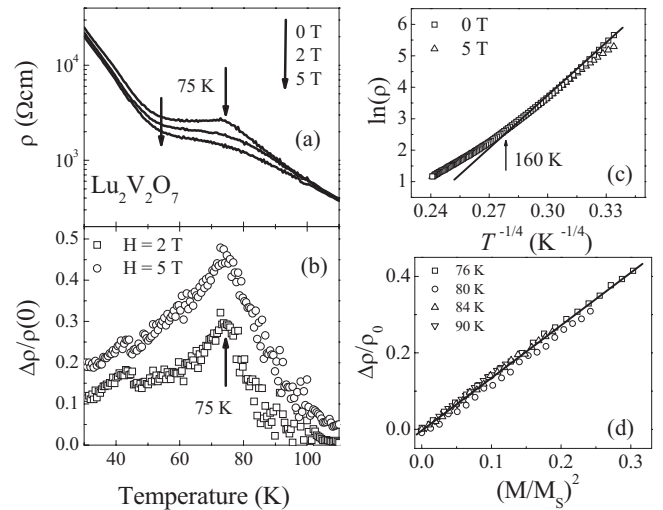


FIG. 3. Temperature dependences of (a) resistivity and (b) magnetoresistance at different magnetic fields for  $\text{Lu}_2\text{V}_2\text{O}_7$ , (c)  $\ln(\rho)$  vs  $T^{-1/4}$  at high temperatures, and (d) dependence of the magnetoresistance as a function of  $(M/M_{\text{sat}})^2$  for several temperatures above  $T_C$ .

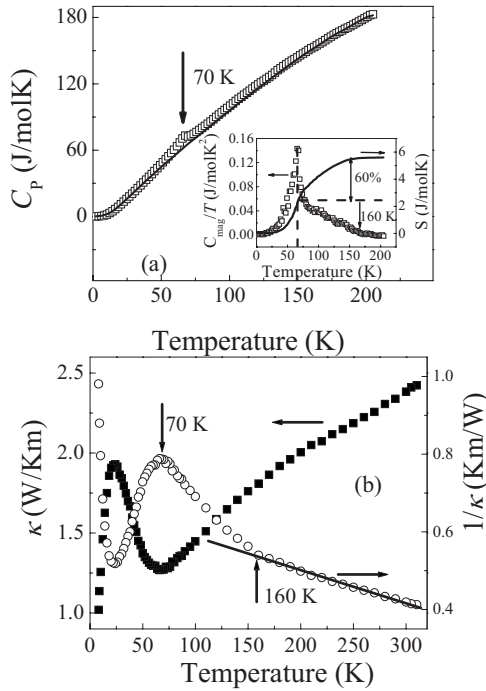


FIG. 4. Temperature dependences of (a) specific heat (open circles,  $\text{Lu}_2\text{V}_2\text{O}_7$ ; solid line,  $\text{Lu}_2\text{Ti}_2\text{O}_7$ ) and (b) thermal conductivity and its inverse for  $\text{Lu}_2\text{V}_2\text{O}_7$ . Inset of (a): temperature dependences of the magnetic specific heat and the calculated entropy for  $\text{Lu}_2\text{V}_2\text{O}_7$ .

polarons within a temperature regime close to  $T_C$ . Above  $T_C$  the MR should exhibit a quadratic dependence on the magnetization:<sup>9</sup>

$$\Delta\rho = [\rho(0) - \rho(H)]/\rho(0) = C(M/M_{\text{sat}})^2, \quad (2)$$

where  $M$  and  $M_{\text{sat}}$  are the magnetization and saturation magnetization, respectively. The temperature-independent scaling factor  $C \approx n^{-2/3}$  is related to the density of charge carriers ( $n$ ) per magnetic unit cell. The magnetization and field dependences of the resistivity were measured at several temperatures (76 K, 80 K, 84 K, and 90 K). The  $\Delta\rho \propto (M/M_{\text{sat}})^2$  curves [Fig. 3(d)] indeed show linear behavior and the slope  $C$  is temperature-independent as predicted by the ML model. The value of  $C=1.5$  here is comparable to that of other ferromagnets, such as  $(\text{FeCu})\text{Cr}_2\text{S}_4$  (Refs. 7 and 18) and  $\text{La}_{1-x}\text{Sr}_x\text{CoO}_3$  (Ref. 19).

The specific heat and thermal conductivity measurements of  $\text{Lu}_2\text{V}_2\text{O}_7$  (Fig. 4) both show a transition at  $T_C \approx 70$  K, which is below the temperature  $T_2=75$  K where the maximum MR occurs. One could argue that the mechanism for the enhanced MR near  $T_C$  is due to the scattering of carriers from enhanced spin fluctuations. However, the expected MR from this effect is very small, on the order of a few percent,<sup>1</sup> and this can be discarded from our analysis. In order to properly determine  $T_C$  to confirm the separation between  $T_C$  and  $T_2$ , the analysis of the spontaneous magnetization  $M_s$  and the initial susceptibility  $\chi_0$  is performed based on the  $M$ - $H$  curve measurements [Fig. 2(c)]. In the region around the magnetic phase transition,  $M_s$  and  $\chi_0$  can be expressed as<sup>20</sup>

$$(\chi_0)^{-1}(T) \propto (T - T_C)^\gamma \quad \text{for } T_C < T, \quad (3)$$

$$M_s(H) \propto H^\delta \quad \text{for } T_C = T, \quad (4)$$

$$M_s(T) \propto (T_C - T)^\beta \quad \text{for } T_C > T. \quad (5)$$

The modified Arrott plot technique<sup>21</sup> was used to determine  $T_C$ ,  $\beta$ ,  $\gamma$ , and  $\delta$  for  $M_s$  and  $1/\chi_0$ . The  $M_s$  as a function of the temperature is determined from the intersection of the linear extrapolation of the straight line in the modified Arrott plots with the  $M^{1/\beta}$  axis, while  $1/\chi_0$  corresponds to the intersection of these lines with the  $(H/M)^{1/\gamma}$  axis. These data are fitted to the exponential behaviors of Eqs. (1) and (3). Figure 2(d) shows the optimum fitting with  $\beta=0.42$ ,  $\gamma=1.85$ , and  $T_C=69.5$  K.  $\delta$  is calculated from the Widom scaling relation  $\delta=1+\gamma/\beta=5.41$ , which is close to the value of  $\delta=5.3$  obtained by the direct fit of  $\delta$  taking into account that, near  $T_C$ ,  $M_s \approx H^\delta$ .<sup>20</sup> The values of  $\beta$ ,  $\gamma$ , and  $\delta$  obtained here are close to those of the Heisenberg model ( $\beta=0.36$ ,  $\gamma=1.39$ , and  $\delta=4.8$ ) for a three-dimensional isotropic ferromagnet.<sup>22,23</sup>

It is clear that  $T_2=75$  K  $\approx 1.1T_C$  is followed by the magnetic transition ( $T_C=69.5$  K) in  $\text{Lu}_2\text{V}_2\text{O}_7$ .  $T_2$ , where the maximum MR occurs, could be related to the temperature where correlations among the magnetic polarons occur. After the ferromagnetic transition at  $T_C$ , magnetic polarons should be delocalized from the self-trapped state and turned into naked carriers, which will induce an abrupt decrease of the resistivity. However, in  $\text{Lu}_2\text{V}_2\text{O}_7$ , the resistivity decreases gradually from 75 K to 60 K, and MR exists in a broad temperature region below  $T_C$ . These behaviors show that magnetic polarons still exist below the ferromagnetic transition but they are decoupled below 60 K. The magnetic polarons and naked carriers coexist in the temperature region between 60 K and  $T_C$ . This is the physical picture that has been developed to describe the MR in  $\text{Ti}_2\text{Mn}_2\text{O}_7$ .<sup>9</sup> The magnetic polarons begin to form at 160 K, where there are deviations from the VRH model resistivity and  $1/\chi$  deviates from linearity in the dc susceptibility. This argument also is supported by the specific heat ( $C_p$ ) and thermal conductivity [ $\kappa(T)$ ] measurements as shown below.

In order to isolate the magnetic contribution to the specific heat  $\text{Lu}_2\text{V}_2\text{O}_7$ , nonmagnetic  $\text{Lu}_2\text{Ti}_2\text{O}_7$  was synthesized and measured. The resultant magnetic specific heat ( $C_{\text{mag}}$ ) (calculated by treating the specific heat of nonmagnetic  $\text{Lu}_2\text{Ti}_2\text{O}_7$  as the lattice contribution) is plotted as  $C_{\text{mag}}/T$  in the inset of Fig. 4(a). The calculated magnetic entropy  $S=5.2$  J/(mol K) is comparable to  $5.8$  J/(mol K)  $= R \ln(2)$ . The anomalous behavior of  $C_{\text{mag}}$  begins at high temperatures (around 160 K), and the calculated fraction of entropy loss above  $T_C$  in the total magnetic entropy denoted as  $S(>T_C)/S$  is around 60%. This large release of entropy above  $T_C$  arises from the formation of magnetic polarons above  $T_C$ .  $\kappa(T)$  of  $\text{Lu}_2\text{V}_2\text{O}_7$  shows several features: (i) At high temperatures  $\kappa(T)$  shows a positive temperature dependence typical of heat transport in an amorphous solid. This behavior obviously deviates from the  $1/T$  law at high temperatures (usually for  $T > \theta_D/4$ ) described by the Debye model for the phonon contribution,<sup>24</sup> but is similar to that of other materi-

als with geometrically frustrated spin arrangements. For example, the  $\kappa(T)$  of hexagonal  $\text{HoMnO}_3$ , with triangular Mn spin arrangements in the  $ab$  plane also shows a glassy behavior in the paramagnetic region due to enhanced spin fluctuations.<sup>25</sup> (ii)  $\kappa(T)$  shows an additional suppression of the glass thermal conductivity between 70 K and 160 K, Fig. 4(b), which is consistent with formation of magnetic polarons observed by magnetic and specific heat measurements in this temperature region. (iii) Below  $T_C=70$  K, the long-range magnetic ordering gives the dramatic restoration of a phonon contribution.

In summary,  $\text{Lu}_2\text{V}_2\text{O}_7$  shows a ferromagnetic transition at  $T_C=69.5$  K and negative MR as high as 50% ( $H=5$  T) around 75 K with weak spin-carrier-lattice couplings. This is the second known pyrochlore other than  $\text{Tl}_2\text{Mn}_2\text{O}_7$  which has strong MR in the absence of a Jahn-Teller-like distortion characteristic of the double-exchange mechanism. One key difference between the two materials is that the mechanism

for polaron formation in  $\text{Tl}_2\text{Mn}_2\text{O}_7$  is believed to be an interaction of the  $d$  electrons of the Mn spins with the  $s$  electrons associated with the  $\text{Ti}^{3+}$  ion. In the case of  $\text{Lu}_2\text{V}_2\text{O}_7$ , the  $\text{Lu}^{3+}$  ion does not have this extended  $s$ -electron shell to assist with polaron formation. This suggests that the route to magnetoresistance in  $\text{Lu}_2\text{V}_2\text{O}_7$  may be distinct from  $\text{Tl}_2\text{Mn}_2\text{O}_7$  and is worth further study for an understanding of this phenomenon.

This work utilized facilities supported in part by the NSF under Agreement No. DMR-0084173, NSF Grant No. DMR-0504769, and DOE Grant No. DE-FG-06ER46269. J.A.S. is supported by CNPq Grant No. 201017/2005-9. A portion of this work was made possible by the NHMFL IHRP, the Schuller Program, the EIEG program, and the State of Florida. The authors would like to acknowledge J. S. Zhou at the University of Texas (Austin) for the thermal conductivity measurements.

\*cwiebe@magnet.fsu.edu

<sup>1</sup>A. P. Ramirez, J. Phys.: Condens. Matter **9**, 8171 (1997).

<sup>2</sup>M. B. Salamon and M. Jaime, Rev. Mod. Phys. **73**, 583 (2001).

<sup>3</sup>M. Imada, A. Fujimori, and Y. Tokura, Rev. Mod. Phys. **70**, 1039 (1998).

<sup>4</sup>M. A. Subramanian, B. H. Toby, A. P. Ramirez, W. J. Marshall, A. W. Sleight, and G. H. Kwei, Science **273**, 81 (1996).

<sup>5</sup>Y. Shimakawa, Y. Kubo, and T. Manako, Nature (London) **379**, 53 (1996).

<sup>6</sup>H. Y. Hwang and S. W. Cheong, Nature (London) **389**, 942 (1997).

<sup>7</sup>A. P. Ramirez, R. J. Cava, and J. Krajewski, Nature (London) **386**, 156 (1997).

<sup>8</sup>Y. Shimakawa, Y. Kubo, T. Manako, Y. V. Sushko, D. N. Argyriou, and J. D. Jorgensen, Phys. Rev. B **55**, 6399 (1997).

<sup>9</sup>P. Majumdar and P. B. Littlewood, Nature (London) **395**, 479 (1998).

<sup>10</sup>P. Majumdar and P. B. Littlewood, Phys. Rev. Lett. **81**, 1314 (1998).

<sup>11</sup>B. Martínez, R. Senis, J. Fontcuberta, X. Obradors, W. Cheikh-Rouhou, P. Strobel, C. Bougerol-Chaillout, and M. Pernet, Phys. Rev. Lett. **83**, 2022 (1999).

<sup>12</sup>L. Soderholm and J. E. Greedan, Mater. Res. Bull. **17**, 707 (1982).

<sup>13</sup>S. Shamoto, T. Nakano, Y. Nozue, and T. Kajitani, J. Phys. Chem. Solids **63**, 1047 (2002).

<sup>14</sup>S. Shamoto, H. Tazawa, Y. Ono, T. Nakano, Y. Nozue, and T. Kajitani, J. Phys. Chem. Solids **62**, 325 (2001).

<sup>15</sup>G. T. Knoke, A. Niazi, J. M. Hill, and D. C. Johnston, Phys. Rev. B **76**, 054439 (2007).

<sup>16</sup>P. G. Radaelli, D. E. Cox, M. Marezio, S. W. Cheong, P. E. Schiffer, and A. P. Ramirez, Phys. Rev. Lett. **75**, 4488 (1995).

<sup>17</sup>J. M. De Teresa, M. R. Ibarra, P. A. Algarabel, C. Ritter, C. Marquina, J. Blasco, J. Garcia, A. del. Moral, and Z. Arnold, Nature (London) **386**, 256 (1997).

<sup>18</sup>Z. Yang, S. Tan, Z. Chen, and Y. Zhang, Phys. Rev. B **62**, 13872 (2000).

<sup>19</sup>S. Yamaguchi, H. Taniguchi, H. Takagi, T. Arima, and Y. Tokura, J. Phys. Soc. Jpn. **64**, 1885 (1995).

<sup>20</sup>H. Eugene Stanley, *Introduction to Phase Transitions and Critical Phenomena* (Oxford University Press, New York, 1971), p. 39.

<sup>21</sup>A. Arrott and J. E. Noakes, Phys. Rev. Lett. **19**, 786 (1967).

<sup>22</sup>K. Ghosh, C. J. Lobb, R. L. Greene, S. G. Karabashev, D. A. Shulyatev, A. A. Arsenov, and Y. Mukovskii, Phys. Rev. Lett. **81**, 4740 (1998).

<sup>23</sup>M. Seeger, S. N. Kaul, H. Kronmüller, and R. Reisser, Phys. Rev. B **51**, 12585 (1995).

<sup>24</sup>R. Berman, *Thermal Conduction in Solids* (Clarendon Press, Oxford, 1976).

<sup>25</sup>H. D. Zhou, J. Lu, R. Vasic, B. W. Vogt, J. A. Janik, J. S. Brooks, and C. R. Wiebe, Phys. Rev. B **75**, 132406 (2007).